Thermodynamics of Formation of Porous Polymeric Membrane by Phase Separation Method I. Nucleation and Growth of Nuclei

Kenji KAMIDE*, Hideki IIJIMA, and Shigenobu MATSUDA

*Fundamental Research Laboratory of Natural and Synthetic Polymers,
Asahi Chemical Industry Co., Ltd.,
11–7 Hacchonawate, Takatsuki, Osaka 569, Japan*

ABSTRACT: An attempt was made to clarify a general principal describing the steps of nucleation to the growth of the primary particles, based on the thermodynamics of phase equilibrium of mono-dispersed polymer/single solvent systems. Activation energy of formation of critical nucleus $\Delta\phi_{CN}$ and radius of the critical nucleus S_{CN} were calculated by using the free energy change due to coagulation per unit volume Δf_v and interfacial free energy between polymer-rich and -lean phases σ on various phase separation points located within the metastable region of phase diagrams. S_{CN} of critical nucleus generated near a cloud point curve was larger than those near a spinodal curve, but $\Delta\phi_{CN}$ became smaller when the phase separation occurred near the spinodal curve, indicating that nucleation tends to occur much more easily near the spinodal curve. Nuclei thus formed and passed though a potential barrier are considered to be in equilibrium with the region surrounded by the local solution spheres of polymer-lean phase. The spheres having radii of S_0 are surrounded by an outer original bulk solution. Growth rate of growing particles were obtained in the isothermal process by solving the general equation of diffusion of polymer molecules from the outer phase. When the phase separation of whole system is attained at time t_P, all the nuclei are conventionally defined as the primary particles. By combining the rate of production of critical nuclei and the total volume of S_0 spheres including growing particles, t_P was determined and distribution of those primary particles was calculated.
    KEY WORDS   Phase Separation / Nucleation / Activation Energy / Interfacial Free Energy / Local Equilibrium / Diffusion / Primary Particle / Porous Polymeric Membrane /

Solvent-casting method is now the most commonly used for preparing the porous polymeric membranes and utilizes the phase separation phenomena of polymer solutions as its basic tenet. The membranes prepared by this method are often composed of the polymer particles as skeleton structure, regardless of their pore sizes. It is clarified by electron micrography (EM) that even reverse osmosis membranes are composed of fine polymer particles.[1,2]

Establishment of underlying principle in the

preparation of porous polymeric membranes by the solvent-casting method is unquestionably important in both aspects of science and industry. Kesting,[3] Smolders,[4] and Pusch[5] attempted to give very qualitative explanation for mechanism of formation of unsymmetric membranes.

Kamide *et al.* made a pioneering work on the relation between the casting conditions and the pore characteristics for cellulose acetate membrane, showing that when cooled down or mixed with poor solvent or solvents mixture

---

* To whom all correspondence should be addressed.

the polymer solution separated into two liquid phases by nucleation mechanism and the trace of the primary particles of polymer-lean phase were detected by EM in the polymer particles constituting dry membranes.[6] From these, it was demonstrated that the polymer particles constituting the back-bone structure of membranes are the secondary particles, grown from the primary particles in the casting process. Kamide *et al.* named "Micro-phase separation method" for the method, in which fine polymer-rich phase particles are formed by phase separation of polymer solutions, proposing rather tentative, but quantitative theory for the mechanism of membrane structure formation by solvent-cast method.[7] In addition, Kamide and his coworkers observed by EM the ultra-thin sections, sliced parallel to the surface of cellulose and cellulose acetate membranes, prepared by the micro-phase separation method, showing that the cellulose and cellulose acetate membranes evidently consist of the small spherical particles having a radius (S_2) of about 0.2 μm and the morphology, including pore radius distribution varies continuously with the distance from the membrane surfaces.[8]

In a series of articles, we attempted to establish a more rigorous and generalized theory of thermodynamics on the formation of porous polymeric membranes.

The process of membrane formation can be divided into several elementary steps as shown in Figure 1. Depending on the initial (overall) polymer concentration [*i.e.*, the solution concentration at the instance of phase separation, which should be strictly distinguished from the polymer concentration of the starting (in this case, casting) solution, v_p^s] v_p^0, either the polymer-rich phase or the polymer-lean phase will initially separates as the dispersed phase from the solution.

If $v_p^0 < v_p^c$ (the critical solution concentration), the polymer-rich phase separated as small particles suspended in a medium (*i.e.*, polymer-lean phase), and these particles grow by amalgamation. The interstitial space between particles gives pore (non-circular pore) (Figures 1b—1j).

When v_p^0 is larger than v_p^c, the polymer-lean phase is separated as shown in Figures 1b'—1j'. Since this phase has a comparatively low viscosity, the particles of the polymer-lean phase gradually become larger by amalgamation. The aggregated polymer-lean phase particles are themselves circular, smooth pores. Even in this case, stage (g') in Figure 1 should be stable in order to prepare the microporous membrane. Figures 1b'—1j' strongly suggests that the circular pores will be formed from
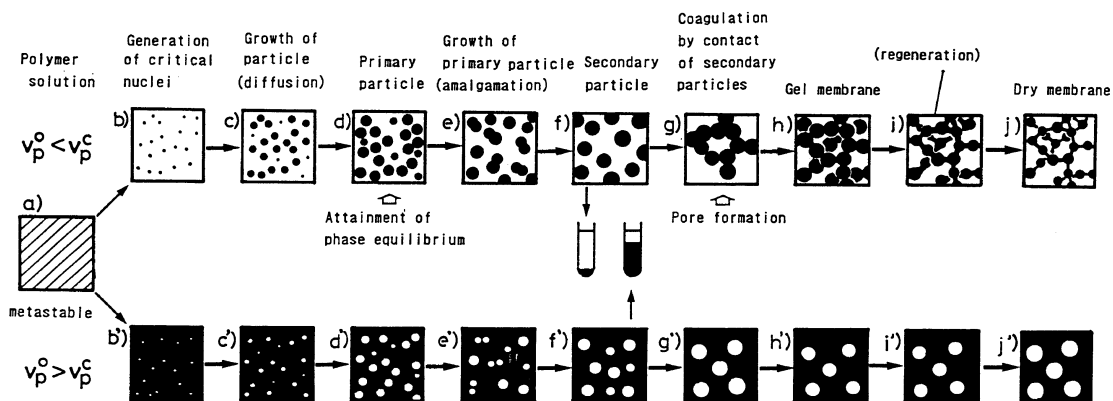

Figure 1. Elementary steps in porous polymeric membrane formation by the micro-phase separation method: v_p^0, polymer volume fraction of the solution when the phase separation occurs; v_p^c, polymer volume fraction of critical solution point.

concentrated solution.

In this article, we intend to clarify a general principle describing the steps of the nucleation to the growth of the primary particles, based on the thermodynamics of phase equilibrium of multicomponent polymer-solvent system. In other words, we attempted to elucidate (1) the mechanism of nucleation from homogeneous solution, (2) the mechanism of growth from critical nuclei to primary particles, (3) the time at which the phase separation of the whole system is attained, and (4) distribution of radius of the primary particle.

THEORY

Generation of Critical Nuclei (Step b)

Before examining the details of the theory, a general explanation of the mechanism of nucleation from the polymer solution will be first presented. The generation and growth of polymer particles (nucleus) by phase separation from homogeneous solution are principally based on the same principle as the condensation of liquid droplets from super-saturated vapors or the formation of ice particles from super-cooled liquids: In homogeneous polymer so-

lutions in the metastable region of the phase diagram (points G or G' in Figure 2) critical nuclei having radius of S_{CN} (see, eq 15), are formed by "concentration fluctuation" and can grow further in size spontaneously. The generation of the precipitated nuclei is always time-retarded and the nuclei thus formed grow by passing through a potential barrier (see, Figure 5). On the other hand, under adequate conditions passing through the critical point, the precipitation occurs instantly because of lack in potential barrier: This is spinodal decomposition.[9]

Figure 2 shows the cloud point curve (full line), spinodal curve (broken line), and critical solution point (open circle) for monodisperse polymer (X-mer)/single solvent system and Figure 3 shows Gibbs' free energy change ΔG_v per unit volume at a given temperature T_P for X-mer/single solvent system. $v_{X(1)}$ and $v_{X(2)}$ are the polymer volume fractions of the polymer-lean and -rich phases in equilibrium and $v_{X(1)}^{SP}$ and $v_{X(2)}^{SP}$ are spinodal concentrations. In the figure, points A and B are two-phase equilibrium points and points C and D are spinodal points. If the initial polymer concentration v_X^0 for monodispersed X-mer lies at T_P between $v_{X(1)}$ and $v_{X(2)}$, the two-phase separation occurs. When v_X^0 lies between $v_{X(1)}$
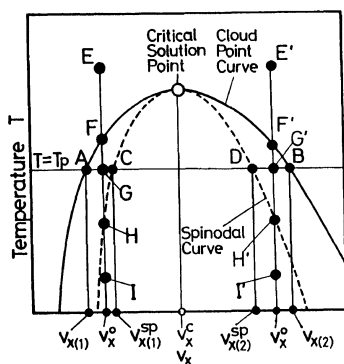

Figure 2. Cloud point curve (solid line), spinodal curve (broken line) and critical solution point (open circle) of monodisperse polymer/solvent system: A and B, coexisting points (at $T = T_P$; T_r, phase separation temperature); C and D, spinodal points ($T = T_P$); E and E′, one phase points; F and F′, cloud point; G and G′, metastable one phase points; H and H′, spinodal points ($v = v_X^0$); I and I′, unstable points.
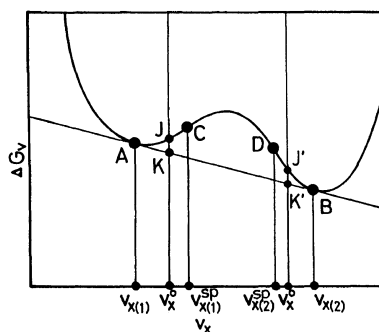

Figure 3. Gibbs' free energy change ΔG_v (eq 3) per unit volume at a given temperature T_P for monodisperse polymer/solvent system: A and B, coexisting points; C and D, spinodal points; J and J′, metastable one phase points; K and K′, points of average free energy of two coexisting phases.

and $v_{X(1)}^{SP}$ or between $v_{X(2)}^{SP}$ and $v_{X(2)}$, the polymer solution can exist as a metastable single phase, from which two-phase separation is initiated by formation of nuclei. In this sense, the spinodal concentration is the upper limit (or lower limit) of concentration, below (or above) which the solution can exist as a metastable single phase for $v_X^0 < v_X^c$ (v_X^c, critical polymer volume fraction) (or for $v_X^0 > v_X^c$). When the polymer solutions at point E (in Figure 2) are cooled down to point F on cloud point curve, nuclei with a radius of S_{CN} (see, eq 17) are formed by thermal fluctuation, which can be

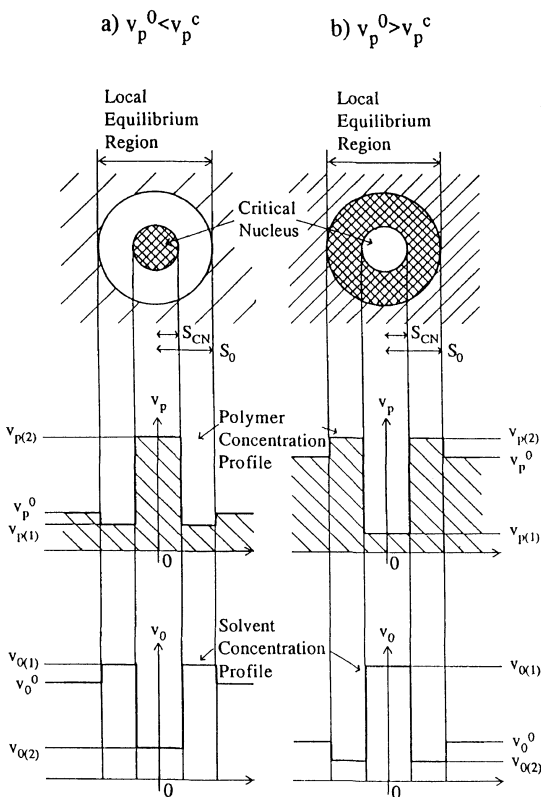a) $v_p^0 < v_p^c$ b) $v_p^0 > v_p^c$

Figure 4. Local equilibrium region and concentration profile of critical nuclei: a) initial (overall) polymer volume fraction of the solution when the phase separation occurs $v_p^0 <$ polymer volume fraction of critical solution point v_p^c, b) $v_p^0 > v_p^c$; $v_{p(1)}$ and $v_{p(2)}$; polymer volume fractions of polymer-lean and -rich phases; $v_{0(1)}$ and $v_{0(2)}$, solvent volume fractions of polymer-lean and -rich phases ($v_{0(1)} = 1 - v_{p(1)}$ and $v_{0(2)} = 1 - v_{p(2)}$); S_{CN}, radius of critical nucleus; S_0, radius of local equilibrium region.

regarded as concentration fluctuation only and a nucleus thus formed is considered to be in equilibrium with the region immediately surrounded by the local solution (polymer-lean phase), which can be approximated as a sphere with a radius of S_0 (see, eq 11c). In the case of $v_X^0 > v_X^c$, the critical nucleus with the radius of S_{CN} generates according to cooling the polymer solution from point E' to point F' and is surrounded by the region of a sphere S_0, mentioned above. Figures 4a and 4b show local equilibrium region and concentration profile of critical nuclei in the case of $v_X^0 < v_X^c$ and $v_X^0 > v_X^c$, respectively. Here, $v_0^0 (= 1 - v_X^0)$ is the initial concentration of the solvent and $v_{0(1)}$ ($= 1 - v_{X(1)}$) and $v_{0(2)}$ ($= 1 - v_{X(2)}$) are the solvent volume fractions of polymer-lean and -rich phases, respectively. The extent of nucleation depends strongly on the time period spent between points F and H (or F' and H'). H and H' are the points on the spinodal curve. For a given polymer solution, cloud point curve, the spinodal curve and critical solution point can be unambiguously calculated.[10-13]

Consider first the isothermal process. The activation energy of formation of a nucleus with the radius S, $\Delta\phi(S)$ is expressed in the same form as derived for nucleation from polymer melt[14]:

$$\Delta\phi(S) = \frac{4}{3}\pi S^3 \Delta f_v + 4\pi S^2 \sigma \qquad (1)$$

where Δf_v is the free energy change of coagulation per unit volume, and is defined as the difference between average Gibbs' free energy of coexisting phases A and B, $\Delta\bar{G}(v_X^0)$ (points K or K' in Figure 3) and Gibbs' free energy change of mixing per unit volume $\Delta G_v(v_X^0)$ (points J or J' in Figure 3; metastable phase), given by

$$\Delta f_v = \Delta\bar{G}(v_X^0) - \Delta G_v(v_X^0) \qquad (2)$$

and σ is the interfacial energy between nucleus and its surroundings. ΔG_v for single phase (e.g., points A, B, C, D, J, and J' in Figure 3) of monodisperse polymer/single

solvent system is

$$\Delta G_v = v_0 \frac{\Delta \mu_0}{V_0} + v_X \frac{\Delta \mu_X}{X V_0}$$

$$= \left(\frac{\tilde{R} T}{V_0} \right) \left[(1 - v_X) \ln(1 - v_X) + \frac{v_X \ln v_X}{X} \right.$$

$$+ \chi_0 \left\{ (v_X - v_X^2) + \frac{p_1}{2} (v_X - v_X^3) \right.$$

$$\left. \left. + \frac{p_2}{3} (v_X - v_X^4) \right\} \right] \tag{3}$$

where $\Delta \mu_0$ and $\Delta \mu_X$ are the modified Flory–Huggins type chemical potentials of solvent and polymer (i.e., X-mer),[10-13] given by the following equations, respectively,

$$\Delta \mu_0 = \tilde{R} T \left[\ln v_0 + \left(1 - \frac{1}{X} \right) v_X \right.$$

$$\left. + \chi_0 (1 + p_1 v_X + p_2 v_X^2) v_X^2 \right] \tag{4}$$

$$\Delta \mu_X = \tilde{R} T \left[\ln v_X - (X - 1)(1 - v_X) \right.$$

$$+ X \chi_0 (1 - v_X)^2 \left\{ 1 + \frac{p_1}{2} (1 + 2v_X) \right.$$

$$\left. \left. + \frac{p_2}{3} (1 + 2v_X + 3v_X^2) \right\} \right] \tag{5}$$

and V_0 is the molar volume of solvent, $\tilde{R}$, the gas constant, T, Kelvin temperature, χ_0, the polymer-solvent interaction parameter at infinite dilution, p_1 and p_2, 1st and 2nd order concentration-dependence parameters of thermodynamic interaction parameter between solvent and polymer, χ.[10-13] χ is given by

$$\chi = \chi_0 (1 + p_1 v_X + p_2 v_X^2) . \tag{6}$$

The coordinates of the points A and B [$(v_{X(1)}, \Delta G_v(v_{X(1)}))$ and $(v_{X(2)}, \Delta G_v(v_{X(2)}))$] are determined first by applying eq 4 and 5 into the Gibbs' conditions for two-phase equilibrium eq 7 and 8, respectively,[10-13]

$$\Delta \mu_{0(1)} = \Delta \mu_{0(2)} \tag{7}$$

$$\Delta \mu_{X(1)} = \Delta \mu_{X(2)} \tag{8}$$

and by substituting $v_{X(1)}$ and $v_{X(2)}$ thus calculated into eq 3.

$\Delta \bar{G}(v_X^0)$ at point $K(v_X^0, \Delta \bar{G}(v_X^0))$ is given by the relation,

$$\Delta \bar{G}(v_X^0) = \frac{\Delta G_v(v_{X(2)}) - \Delta G_v(v_{X(1)})}{v_{X(2)} - v_{X(1)}} (v_X^0 - v_{X(1)})$$

$$+ \Delta G_v(v_{X(1)}) . \tag{9}$$

Then, substituting eq 3 and 9 into eq 2, Δf_v can be straightforwardly calculated.

Of course, between the phase volume ratio R, v_X^0, $v_{X(1)}$, and $v_{X(2)}$ the relation

$$R \equiv \frac{V_{(1)}}{V_{(2)}} = \frac{v_{X(2)} - v_X^0}{v_X^0 - v_{X(1)}} \tag{10}$$

holds. Here, $V_{(1)}$ and $V_{(2)}$ are the volumes of the polymer-lean and -rich phases, respectively. We adopt the hypothesis that thermodynamic equilibrium is attained between the nucleus $(0 < S < S_{CN})$ and its surrounding sphere $(S_{CN} < S < S_0$; S_0, radius of local equilibrium region), but there is no equilibrium between the sphere and its outer large homogeneous phase $(S > S_0)$ (Figure 4). However, note that this hypothesis (i.e., "local equilibrium hypothesis") has not yet been fully verified experimentally. When "local equilibrium hypothesis" is accepted, $V_{(1)}$, $V_{(2)}$, and R are given by the formula:
In the case of $v_X^0 < v_X^c$

$$V_{(1)} = \frac{4}{3} \pi (S_0^3 - S_{CN}^3) , \tag{11a}$$

$$V_{(2)} = \frac{4}{3} \pi S_{CN}^3 , \tag{11b}$$

$$R = \frac{S_0^3 - S_{CN}^3}{S_{CN}^3} . \tag{11c}$$

In the case of $v_X^0 > v_X^c$

$$V_{(1)} = \frac{4}{3} \pi S_{CN}^3 , \tag{12a}$$

$$V_{(2)} = \frac{4}{3}\pi(S_0^3 - S_{CN}^3), \qquad (12b)$$

$$R = \frac{S_{CN}^3}{S_0^3 - S_{CN}^3}. \qquad (12c)$$

Coordinates of the spinodal points C and D $[(v_{X(1)}^{SP}, \Delta G_v(v_{X(1)}^{SP}))$ and $(v_{X(2)}^{SP}, \Delta G_v(v_{X(2)}^{SP}))]$ can be calculated by solving the equation[13]

$$\frac{1}{1-v_X} + \frac{1}{Xv_X} - \chi_0(2 + 3p_1v_X + 4p_2v_X^2) = 0 \qquad (13)$$

for a given χ_0. And the critical solution point (v_X^c, χ_0^c) can be evaluated by solving the simultaneous equations (eq 13 and 14).[13]

$$\frac{1}{(1-v_X)^2} - \frac{1}{Xv_X^2} - \chi_0(3p_1 + 8p_2v_X) = 0. \quad (14)$$

The above discussion on monodisperse polymer/solvent system can easily be extended to more general systems including polydisperse polymer/solvent/nonsolvent system.

Evidently, $\Delta\phi$ is a function of S as illustrated in Figure 5. $\Delta\phi$ of Figure 5 is calculated using $\Delta f_v = -300.99 \, \mathrm{J \, m^{-3}}$ and $\sigma = 3 \times 10^{-6} \, \mathrm{J \, m^{-2}}$. The radius of critical nuclei, S_{CN} is derived by applying the condition of $\partial\Delta\phi/\partial S = 0$ to eq 1 to yield

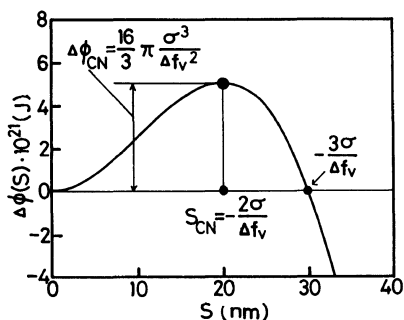$$S_{CN} = -\frac{2\sigma}{\Delta f_v}. \qquad (15)$$

Figure 5. Plot of activation energy of formation of nucleus $\Delta\phi(S)$ as a function of nucleus size S (eq 1): $\Delta f_v = -300.99 \, \mathrm{J \, m^{-3}}$; $\sigma = 3 \times 10^{-6} \, \mathrm{J \, m^{-2}}$; in this case, $S_{CN} \approx 20 \, \mathrm{nm}$ and $\Delta\phi_{CN} \approx 5 \times 10^{-21} \, \mathrm{J}$.

When a nucleus formed at a given instant has a radius S_N larger than S_{CN}, the nucleus will continue to grow spontaneously. The activation energy of formation of critical nucleus $\Delta\phi_{CN}$ is written by combining eq 15 with eq 1 as

$$\Delta\phi_{CN} = \frac{16\pi\sigma^3}{3\Delta f_v^2}. \qquad (16)$$

It should be emphasized that in this case, although the phase equilibrium has not yet been attained over the whole solution system, R for the local equilibrium region surrounding each nucleus is considered to coincide with R for the whole system (eq 10).

Growth of Nucleus (Step c) to Primary Particle (Step d)

The profile of polymer concentration around a nucleus $(v_p^0 < v_p^c)$ is demonstrated in Figure 6. Then, the polymer concentrations of a nucleus, its surrounding sphere and outer homogeneous phase are $v_{p(1)}$, $v_{p(2)}$, and v_p^0, respectively. S_0 is related to R through the relation:

$$R = \frac{S_0^3 - S_{CN}^3}{S_{CN}^3} \left(= \frac{v_{p(2)} - v_p^0}{v_p^0 - v_{p(1)}} \right) \quad \text{for} \quad v_p^0 < v_p^c \qquad (17)$$

$$R = \frac{S_{CN}^3}{S_0^3 - S_{CN}^3} \left(= \frac{v_{p(2)} - v_p^0}{v_p^0 - v_{p(1)}} \right) \quad \text{for} \quad v_p^0 > v_p^c \qquad (18)$$

Of course, $v_{p(1)}$ and $v_{p(2)}$ can be calculated theoretically for any polymer solution.

For $v_p^0 < v_p^c$, after the generation of a nucleus, the polymer molecules in the outer phase, based on the concentration difference $v_p^0 - v_{p(1)}$, immediately diffuse into the sphere (Figure 6b). The number of the polymer molecules diffusing through the unit area of the spherical surface from the outer phase per unit time is given by solving the general equation of diffusion in the form

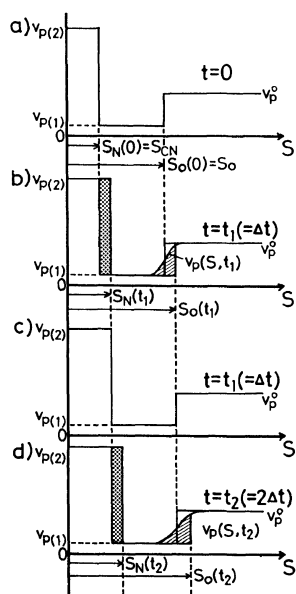$$\frac{\partial v_p}{\partial t} = D\nabla^2 v_p \qquad (19)$$

Figure 6. Concentration profiles of a critical nucleus with a radius of $S_N(t)$ and its surrounding sphere with a radius of $S_0(t)$: a) the profile of polymer concentration around the critical nucleus at $t=0$. $v_{p(2)}$, the polymer concentration of nucleus, $v_{p(1)}$, its surrounding sphere and v_p^0, its outer homogeneous phase; b) increase of the radius of the nucleus (shadowed area) due to diffusion [$v_p(S, t_1)$, hatched area] from the outer phase at $t=t_1$ ($=\Delta t$); c) the profile of polymer concentration around the nucleus at $t=t_1$; d) increase of the radius of the nucleus (shadowed area) due to diffusion [$v_p(S, t_2)$, hatched area] from the outer phase at $t=t_2(=2\Delta t)$.

with

$$V^2 = \frac{1}{S^2}\frac{\partial}{\partial S}\left(S^2\frac{\partial}{\partial S}\right)$$

$$+ \frac{1}{S^2}\left\{\frac{1}{\sin\theta}\frac{\partial}{\partial\theta}\left(\sin\theta\frac{\partial}{\partial\theta}\right)+\frac{1}{\sin^2\theta}\frac{\partial^2}{\partial\psi^2}\right\}$$

$$(20)$$

(θ and ψ are polar coordinates) under the boundary conditions of $v_p(S, 0)=v_{p(1)}$ in the range of $S_{CN}<S<S_0(0)$ and $v_p(S, 0)=v_p^0$ for $S_{CN}>S_0(0)$ (Figure 6a) as[15]

$$v_p(S, t) = (v_p^0 - v_{p(1)})\left[\frac{\phi(S_{0+})+\phi(S_{0-})}{2}\right.$$

$$+ \frac{1}{S}\sqrt{\frac{Dt}{\pi}}\{\exp(-S_{0+}^2)$$

$$\left. -\exp(-S_{0-}^2)\}\right] + v_{p(1)} \qquad (21)$$

where

$$\phi(x) = \frac{2}{\sqrt{\pi}}\int_0^x \exp(-u^2)du, \qquad (22)$$

$$S_{0+} = \frac{S_0+S}{2\sqrt{Dt}}, \qquad (23a)$$

$$S_{0-} = \frac{S_0-S}{2\sqrt{Dt}}. \qquad (23b)$$

Here, $\phi(x)$ is the error function, D, the diffusion coefficient and t, the growing time of nucleus by diffusion. We define $t=0$ as the instant of appearance of a critical nucleus and the concentration profile around the nucleus at $t=t_1$ ($=\Delta t$) is illustrated in Figure 6b. If we can also assume that the thermodynamic equilibrium holds even at $t=t_1$ between the nucleus ($0<S<S_N(t_1)$) and the surrounding sphere ($S_N(t_1)<S<S_0(t_1)$), the diffusion of polymer molecules (hatched area in Figure 6b) from the outer phase into $S_0(0)$ sphere will instantly result in an increase in the radius of the nucleus (shadowed area in Figure 6b) yielding $S_N(t_1)$ [i.e., S_{CN} ($\equiv S_N(0)$)$\rightarrow S_N(t_1)$] (see, Figure 6b). This can be understood as nucleus growth. When the thermodynamic equilibrium between the nucleus and its surrounding sphere holds even at $t=t_2$ ($\equiv 2\Delta t$), the radius of the nucleus increases from $S_N(t_1)$ to $S_N(t_2)$ (Figures 6c and 6d). The concentration profile of diffusion at $t=t_2$, $v_p(S, t_2)$ can be numerically evaluated in this case by solving the diffusion equation (eq 19) under the boundary conditions of $v_p(S, t_1)=v_{p(1)}$ ($S_N(t_1)<S<S_0(t_1)$) and $v_p(S, t_1)=v_p^0$ ($S>S(t_1)$).

The above treatment can be readily extended to the more general case of a nucleus with a radius of $S_N(t_1)$ and its surrounding sphere with a radius of $S_0(t_1)$, obtained at time $t=t_i$ ($\equiv i\Delta t$).

$v_p(S, t_1)$ can be estimated by solving eq 19 under the boundary conditions of $v_p(S, t_{i-1}) = v_{p(1)}$ $(S_N(t_{i-1}) < S < S_0(t_{i-1}))$ and $v_p(S, t_{i-1}) = v_p^0$ $(S > S_0(t_{i-1}))$ when the following relation holds

$$R = \frac{S_0(t_i)^3 - S_N(t_i)^3}{S_N(t_i)^3} \quad (i = 1, 2, 3, \cdots) \quad (24)$$

among $S_N(t_i)$, $S_0(t_i)$ and the phase volume ratio R determined by eq 17.

An increment of polymer volume during $t = t_{i-1}$ and $t = t_i$ in the polymer-lean phase ranging from $S_N(t_{i-1})$ and $S_0(t_i)$, $\Delta V_{p(1)}$ is given by the following equation;

$$\Delta V_{p(1)}(t_i) = 4\pi \int_{S_N(t_{i-1})}^{S_0(t_i)} \{v_p(S, t_i) - v_{p(1)}\} S^2 dS . \tag{25}$$

As the thermodynamics equilibrium is maintained between the nucleus $(0 < S < S_N(t_i))$ and its surrounding sphere $(S_N(t_i) < S < S_0(t_i))$ (in other words, eq 7 and 8 hold), polymer concentration of nucleus and its surrounding sphere should be kept as $v_{p(2)}$ and $v_{p(1)}$, respectively, and increment of the polymer volume in the polymer-rich phase during $t = t_{i-1}$ and $t = t_i$, $|\Delta V_{p(2)}(t_i)|$ is the same as $|\Delta V_{p(1)}(t_i)|$ under the condition given by eq 24. Here, $\Delta V_{p(2)}(t_i)$ is given by

$$\Delta V_{p(2)}(t_i) = \frac{4\pi}{3} v_{p(2)} \{S_N(t_i)^3 - S_N(t_{i-1})^3\} \tag{26}$$

and combining eq 25 and 26, we obtain

$$S_N(t_i)^3 = \frac{3}{v_{p(2)}} \int_{S_N(t_{i-1})}^{S_0(t_i)} (v_p(S, t_i) - v_{p(1)}\} S^2 dS$$
$$+ S_N(t_{i-1})^3 . \tag{27}$$

Solving the integral equation eq 27 under the conditions of eq 24, $S_N(t_i)$ and $S_0(t_i)$ are obtained.

Differentiation of eq 27 with respect to t gives

$$\frac{\partial S_N(t)}{\partial t} = \frac{1}{v_{p(2)} S_N(t)^2} \int_{S_{CN}}^{S_0(t)} \left(\frac{\partial v_p(S, t)}{\partial t}\right) S^2 dS . \tag{28}$$

Equation 28 is an expression giving the growth rate of the nucleus. Kamide and Manabe[7] proposed a somewhat different approach to the estimation of the growth rate using a rather rough approximation. $\partial v(S, t)/\partial t$ in eq 28 can be determined by differentiation of eq 21 with respect to t, in the form:

$$\frac{\partial v_p(S, t)}{\partial t} = (v_p^0 - v_{p(1)})$$

$$\times \left[\frac{1}{2\sqrt{\pi t}} \{S_{0+} \exp(-S_{0+}^2) \right.$$

$$- S_{0-} \exp(-S_{0-}^2)\}$$

$$- \frac{1}{2S} \sqrt{\frac{D}{\pi t}} \{\exp(-S_{0+}^2) - \exp(-S_{0-}^2)\}$$

$$- \frac{1}{S} \sqrt{\frac{D}{\pi t}} (S_{0+}^2 \exp(-S_{0+}^2)$$

$$\left. - S_{0-}^2 \exp(-S_{0-}^2) \right] . \tag{29}$$

RESULTS AND DISCUSSION

Generation of Critical Nuclei (Step b)

Figures 7a and 7b show the cloud point curve (full line) [in a), χ_0^{cp} vs. v_X and in b), cloud point temperature T_{CP} vs. v_X], spinodal curve (broken line) [in a), χ_0^{SP} vs. v_X and in b), T_{SP} vs. v_X] and critical solution point (unfilled circle) in a case of $X = 1 \times 10^2$. Figures 7c and 7d show ΔG_v vs. v_X curve and $-[(\Delta \bar{G} - \Delta G_v)/\tilde{R}T]$ vs. v_X curve, respectively. Here, the calculations were carried out under the following conditions; $p_1 = 0.642$, $p_2 = 0.190$, $\theta = 307.1$ K, $\psi_0 = 0.27$ and $V_0 = 108.74$ cm^3 mol^{-1}. These values except X and V_0 were determined for atactic polystyrene (PS)/cyclohexane (CH) system by analyzing the critical point data through use of Kamide-Matsuda method in 1984.[11] θ and ψ_0 are substituted into eq 30

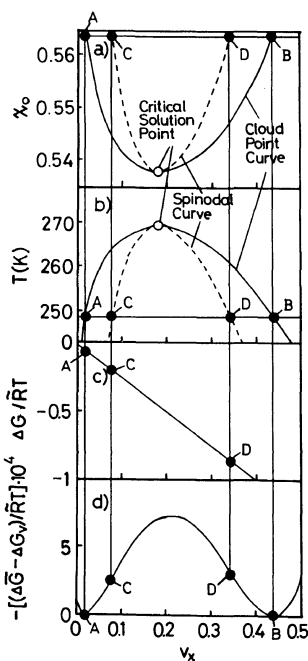$$T = \frac{\psi_0 \theta}{\chi_0 + \psi_0 - 0.5} \tag{30}$$

Figure 7. Cloud point curve (solid line), spinodal curve (broken line) and critical solution point (open circle) of monodisperse polymer/single solvent system [a) χ_0 vs. v_X plot, b) T vs. v_X plot] together with $\Delta G_v/\tilde{R}T$ vs. v_X^0 plot, c) and $-[(\Delta\bar{G}-\Delta G_v)/\tilde{R}T]$ vs. v_X plot, d): Original polymer; monodisperse $(X=1\times10^2)$ and $p_1=0.642$, $p_2=0.190$, $\theta=307.1\,\text{K}$ and $\psi_0=0.27$. $v_X^c=0.1807$ and $\chi_0^c=0.5377$ $(T=269.5\,\text{K})$ and χ_0 (and T) at phase separation point $\chi_0^P=0.5633$ (and $T=248.8\,\text{K}$).

to convert χ_0 to T. The area, surrounded by cloud point curve and spinodal curve is the metastable region where the critical nuclei are formed as previously mentioned. For $X=1\times10^2$, the critical solution point is $v_X^c=0.1807$ and $\chi_0^c=0.5377$ $(T_C=269.47\,\text{K})$ (see, eq 13 and 14). ΔG_v and $\Delta\bar{G}$ were calculated for the phase separation temperature $T_P=248.8\,\text{K}$ (i.e., $\chi_0^P=0.5633$) when $X=1\times10^2$. In this case, the coexisting compositions are $v_{X(1)}=0.02$ (point A) and $v_{X(2)}=0.4368$ (B) and the spinodal compositions are $v_{X(1)}^{SP}=0.0774$ (C) and $v_{X(2)}^{SP}=0.3405$ (D). ΔG_v vs. v_X^0 curve is roughly linear in the range $0<v_X^0<0.5$, but $-(\Delta\bar{G}-\Delta G_v)$ vs. v_X^0 curve has two minimums at points A and B and two inflection points at points C and D (spinodal points).

Figure 8. The cloud point curve (broad solid line), spinodal curve (broken line) and critical solution point (unfilled circle) of monodisperse polymer/single solvent system: $p_1=0.642$, $p_2=0.190$, $\theta=307.1\,\text{K}$ and $\psi_0=0.27$; ●, phase separation point (hypothetical one phase); Arrows indicate phase separation points listed in Tables I and II; a) and d), $X=100$; b) and e), $X=300$; c) and f), $X=1000$.

Wolf and Heinrich[16] measured the interfacial tension (=interfacial free energy) σ between the coexisting phases of the systems cyclohexane/polystyrene and methylcyclohexane/polystyrene and revealed that the knowledge of the chain length of the polymer and of the polymer content in the two coexisting phases suffices to predict the σ between them, at least for typical vinyl polymers. They presented experimentally the generalized equation

$$\sigma(\text{mN m}^{-1})=0.153X^{0.5}(v_{X(2)}-v_{X(1)})^{3.85}$$

$$(31)$$

K. KAMIDE, H. IIJIMA, and S. MATSUDA

where X is the number of monomeric units of the polymer. In the calculation of the size of critical nuclei this equation was employed.

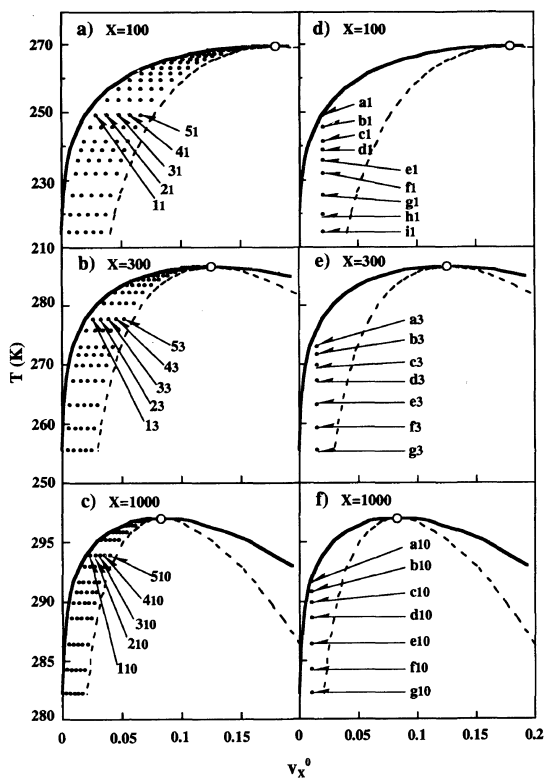Figure 8a shows the phase separation points (*i.e.*, hypothetical metastable single phase, filled circle) as well as the cloud point curve (solid line), spinodal curve (broken line) and critical solution point (unfilled circle) for PS with $X = 1 \times 10^2$/CH. Figures 8b and 8c show results obtained in cases of PS with $X = 3 \times 10^2$ and 1×10^3, respectively. Larger figures of numbers in Figures 8a—8c like 1 of 1_1 or 5 of 5_3, *etc.*

Table I. Size of critical nuclei S_{CN} and activation energy of formation of critical nuclei, $\Delta\phi_{CN}$, of polystyrene (X-mer) solution in cyclohexane: Effect of initial polymer concentration v_X^0.

X	T_P/K	No.[a]	v_X^0	$v_{X(1)}$	$v_{X(2)}$	R	$\Delta f_v/\mathrm{J\,m^{-3}}$	$\sigma/\mathrm{J\,m^{-2}}$	S_{CN}/nm	$\Delta\phi_{CN}/\mathrm{J}$
100	248.8	1_1	0.0296			42.6	-2.67×10^2		394.5	3.43×10^{-17}
		2_1	0.0391			20.8	-9.09×10^2		115.8	2.96×10^{-18}
		3_1	0.0487	0.0200	0.4368	13.5	-1.78×10^3	5.26×10^{-5}	59.3	7.75×10^{-19}
		4_1	0.0582			9.9	-2.78×10^3		37.9	3.17×10^{-19}
		5_1	0.0678			7.7	-3.85×10^3		27.3	1.64×10^{-19}
200	268.9	1_2	0.0276			41.6	-8.63×10		646.8	4.89×10^{-17}
		2_2	0.0352			20.3	-2.98×10^2		187.2	4.10×10^{-18}
		3_2	0.0427	0.0200	0.3431	13.2	-5.89×10^2	2.79×10^{-5}	94.9	1.05×10^{-18}
		4_2	0.0503			9.7	-9.26×10^2		60.3	4.25×10^{-19}
		5_2	0.0579			7.5	-1.29×10^3		43.3	2.19×10^{-19}
300	277.6	1_3	0.0266			40.9	-4.28×10		857.7	5.65×10^{-17}
		2_3	0.0331			19.9	-1.49×10^2		246.1	4.65×10^{-18}
		3_3	0.0397	0.0200	0.2948	13.0	-2.96×10^2	1.83×10^{-5}	124.1	1.18×10^{-18}
		4_3	0.0463			9.5	-4.67×10^2		78.5	4.74×10^{-19}
		5_3	0.0528			7.4	-6.53×10^2		56.2	2.43×10^{-19}
500	286.0	1_5	0.0254			39.8	-1.68×10		1213.6	6.30×10^{-17}
		2_5	0.0308			19.4	-5.92×10		344.8	5.09×10^{-18}
		3_5	0.0363	0.0200	0.2409	12.6	-1.18×10^2	1.02×10^{-5}	172.7	1.28×10^{-18}
		4_5	0.0417			9.2	-1.88×10^2		108.8	5.06×10^{-19}
		5_5	0.0471			7.2	-2.63×10^2		77.6	2.57×10^{-19}
1000	293.8	1_{10}	0.0241			38.1	-4.32		1910.2	6.31×10^{-17}
		2_{10}	0.0282			18.5	-1.54×10		536.2	4.97×10^{-18}
		3_{10}	0.0322	0.0200	0.1795	12.0	-3.10×10	4.13×10^{-6}	266.2	1.22×10^{-18}
		4_{10}	0.0363			8.8	-4.95×10		166.6	4.80×10^{-19}
		5_{10}	0.0404			6.8	-6.98×10		118.3	2.42×10^{-19}
3000	300.8	1_{30}	0.0224			35.1	-3.65×10^{-1}		3755.2	4.05×10^{-17}
		2_{30}	0.0248			17.1	-1.32		1037.8	3.09×10^{-18}
		3_{30}	0.0272	0.0200	0.1068	11.0	-2.69	6.86×10^{-7}	508.9	7.44×10^{-19}
		4_{30}	0.0296			8.0	-4.35		315.5	2.86×10^{-19}
		5_{30}	0.0320			6.2	-6.16		222.5	1.42×10^{-19}
5000	302.6	1_{50}	0.0218			33.7	-9.24×10^{-2}		5118.0	2.59×10^{-17}
		2_{50}	0.0236			16.3	-3.39×10^{-1}		1396.8	1.93×10^{-18}
		3_{50}	0.0253	0.0200	0.0816	10.6	-6.95×10^{-1}	2.36×10^{-7}	680.1	4.58×10^{-19}
		4_{50}	0.0271			7.7	-1.13		419.6	1.74×10^{-19}
		5_{50}	0.0289			1 5.9	-1.60		294.8	8.61×10^{-20}

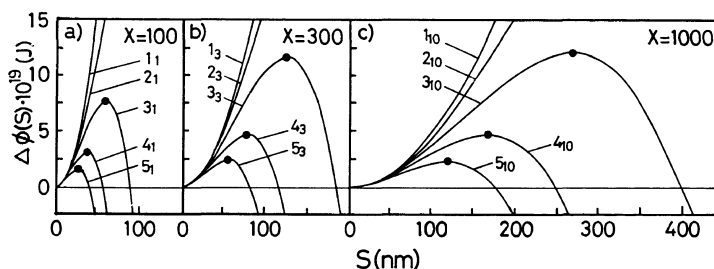[a] Locations in phase diagram for $X = 100$, 300, and 1000 are shown in Figures 8a—8c.

Figure 9. Effect of the free energy change of coagulation per unit volume, Δf_v on the relation between activation energy of formation of nucleus $\Delta\phi(S)$ and nucleus size S at constant interfacial free energy σ between polymer-lean and -rich phases under the following conditions: a), $X=100$; $v_{X(1)}=0.02$; $v_{X(2)}=0.4368$; $\sigma=5.26\times10^{-5}\,\mathrm{J\,m^{-2}}$; 1_1, $v_X^0=0.0296$; $\Delta f_v=-2.67\times10^2\,\mathrm{J\,m^{-3}}$; 2_1, $v_X^0=0.0391$; $\Delta f_v=-9.09\times10^2\,\mathrm{J\,m^{-3}}$; 3_1, $v_X^0=0.0487$; $\Delta f_v=-1.78\times10^3\,\mathrm{J\,m^{-3}}$; 4_1, $v_X^0=0.0582$; $\Delta f_v=-2.78\times10^3$ $\mathrm{J\,m^{-3}}$; 5_1, $v_X^0=0.0678$; $\Delta f_v=-3.85\times10^3\,\mathrm{J\,m^{-3}}$; b), $X=300$; $v_{X(1)}=0.02$; $v_{X(2)}=0.2948$; $\sigma=1.83\times10^{-5}$ $\mathrm{J\,m^{-2}}$; 1_3, $v_X^0=0.0266$; $\Delta f_v=-4.28\times10\,\mathrm{J\,m^{-3}}$; 2_3, $v_X^0=0.0331$; $\Delta f_v=-1.49\times10^2\,\mathrm{J\,m^{-3}}$; 3_3, $v_X^0=0.0397$; $\Delta f_v=-2.96\times10^2\,\mathrm{J\,m^{-3}}$; 4_3, $v_X^0=0.0463$; $\Delta f_v=-4.67\times10^2\,\mathrm{J\,m^{-3}}$; 5_3, $v_X^0=0.0528$; $\Delta f_v=-6.53\times10^2$ $\mathrm{J\,m^{-3}}$; c), $X=1000$; $v_{X(1)}=0.02$; $v_{X(2)}=0.1795$; $\sigma=4.13\times10^{-6}\,\mathrm{J\,m^{-2}}$; 1_{10}, $v_X^0=0.0241$; $\Delta f_v=-4.32\,\mathrm{J\,m^{-3}}$; 2_{10}, $v_X^0=0.0282$; $\Delta f_v=-1.54\times10\,\mathrm{J\,m^{-3}}$; 3_{10}, $v_X^0=0.0322$; $\Delta f_v=-3.10\times10\,\mathrm{J\,m^{-3}}$; 4_{10}, $v_X^0=0.0363$; $\Delta f_v=-4.95\times10\,\mathrm{J\,m^{-3}}$; 5_{10}, $v_X^0=0.0404$; $\Delta f_v=-6.98\times10\,\mathrm{J\,m^{-3}}$; closed circle, $\Delta\phi(S)$ and S of critical nucleus (*i.e.*, $\Delta\phi_{CN}$ and S_{CN}).

correspond to positions where a line between a cloud point and a spinodal point at the constant T_P are divided into six equal parts. Small suffixes (1, 3, and 10) mean $X/100$. Accordingly, 1_1 is the nearest point to a cloud point and 5_1 is the nearest to a spinodal point.

Table I collects the values of Δf_v, σ and S_{CN} which were calculated for PS with $X=1\times10^2$—5×10^3 in CH at $v_{p(1)}=0.0200$. Here, interfacial free energy σ between polymer-lean and -rich phases of PS/CH solution was determined by use of eq 31. The radius of critical nuclei S_{CN} ranges from the order of several thousand nm to several ten nm, decreasing with increase in initial concentration or when the phase separation point comes nearer the spinodal curve. S_{CN} becomes smaller for smaller X. For $X=1\times10^2$ or 2×10^2, S_{CN} had magnitude of the same order as those of the primary particles observed by EM.

Figure 9 shows relation between radius of nuclei S and $\Delta\phi(S)$ at a given phase separation point. Numbers on curves are those (1_1—5_1, 1_3—5_3, and 1_{10}—5_{10}) listed in Table I and are also shown in Figures 8a—8c. S_{CN} of critical nuclei generated near the cloud point curve were larger than those near a spinodal curve,

but $\Delta\phi_{CN}$ became smaller when the phase separation occurred near the spinodal curve, indicating that nucleation tends to occur much more easily near the spinodal curve.

Figures 10a—10d show effects of v_X^0 on R, Δf_v, S_{CN}, and $\Delta\phi_{CN}$ under the phase separation condition, shown as closed circles in Figure 8a. If solutions having different initial polymer concentrations obey to phase separation at the constant temperature, R, Δf_v, S_{CN}, and $\Delta\phi_{CN}$ become smaller at larger v_X^0. Figures 11a—11c show S_{CN} generated at phase separation points as shown in Figures 8a—8c. In the figures, data points for $S_{CN}>500\,\mathrm{nm}$ were omitted.

When a solution is cooled from a single phase state to bring about two-phase separation, the solution passes through the cloud point and Δf_v attains the minimum on the cloud point curve and accordingly, S_{CN} on the cloud point is the maximum. Table II shows results calculated on phase separation points as shown in Figures 8d—8f for PS solutions with $X=1\times10^2$, 3×10^2, and 1×10^3. In these figures, point a is the nearest to the cloud point curve and suffixes (small figures) mean $X/100$. Critical nuclei seldom generate on the cloud point curve and the activation energy of
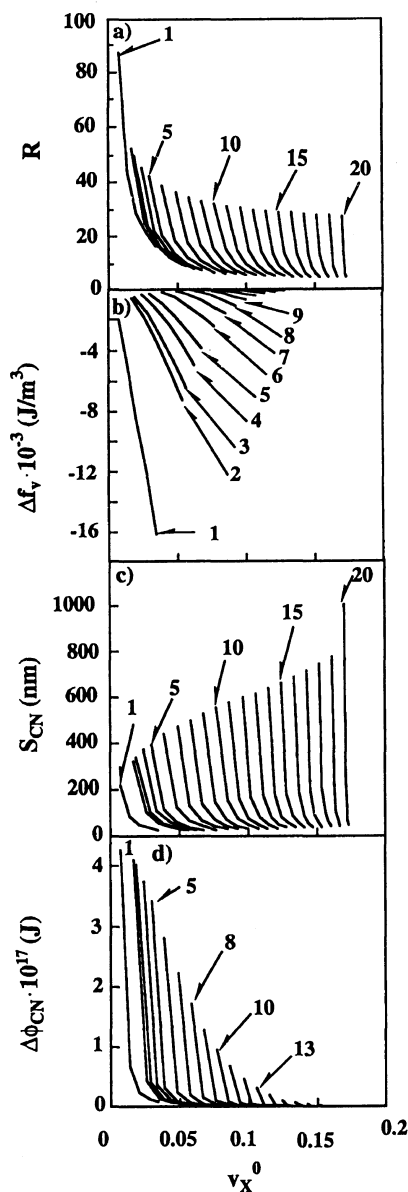
Figure 10. Effects of initial polymer concentration v_X^0 on phase volume ratio $R(a)$, free energy change of coagulation per unit volume Δf_v (b), radius of critical nucleus S_{CN} (c) and activation energy of formation of critical nucleus $\Delta \phi_{CN}$ (d): $X = 100$; numbers mean phase separation temperature T_P; 1, $T_P = 214.4$ K; 2, $T_P = 238.7$ K; 3, $T_P = 241.1$ K; 4, $T_P = 245.5$ K; 5, $T_P = 248.8$ K; 6, $T_P = 253.4$ K; 7, $T_P = 256.8$ K; 8, $T_P = 259.3$ K; 9, $T_P = 261.4$ K; 10, $T_P = 263.0$ K; 11, $T_P = 264.4$ K; 12, $T_P = 265.5$ K; 13, $T_P = 266.4$ K; 14, $T_P = 267.2$ K; 15, $T_P = 267.9$ K; 16, $T_P = 268.4$ K; 17, $T_P = 268.8$ K; 18, $T_P = 269.1$ K; 19, $T_P = 269.3$ K; 20, $T_P = 269.4$ K.
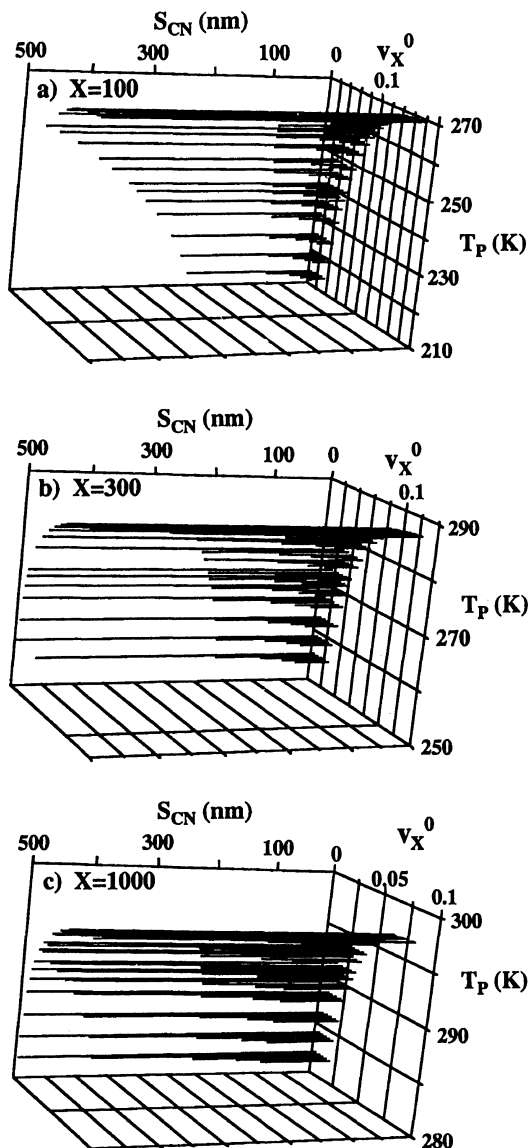
Figure 11. Three dimensional views of relation between radius of critical nucleus S_{CN}, phase separation points (v_X^0 and T_P) on a phase diagram: a), $X = 100$; b), $X = 300$; c), $X = 1000$: Data points of $S_{CN} > 500$ nm are not shown here.

formation of critical nucleus $\Delta \phi_{CN}$ and S_{CN} are the smallest on the spinodal curve.

Growth of Nucleus (Step c) to Primary Particle (Step d)

Figure 12 demonstrates the concentration

Table II. Size of critical nuclei S_{CN} and activation energy of formation of critical nuclei, $\Delta\phi_{CN}$, of polystyrene (X-mer) solutions in cyclohexane: Effect of T_p

X	T_P/K	No.[a]	v_X^0	$v_{X(1)}$	$v_{X(2)}$	R	$\Delta f_v/J\,m^{-3}$	$\sigma/J\,m^{-2}$	S_{CN}/nm	$\Delta\phi_{CN}/J$
	248.8	a_1		0.0200	0.4367	433.8	-3.18	5.26×10^{-5}	33064.8	2.41×10^{-13}
	245.5	b_1		0.0150	0.4567	73.1	-1.52×10^2	6.58×10^{-5}	866.7	2.07×10^{-16}
	241.1	c_1		0.0100	0.4818	42.1	-6.74×10^2	8.49×10^{-5}	252.0	2.26×10^{-17}
100	238.7	d_1	0.0210	0.0080	0.4944	36.5	-1.08×10^3	9.54×10^{-5}	176.7	1.25×10^{-17}
	235.7	e_1		0.0060	0.5094	32.7	-1.70×10^3	1.09×10^{-4}	128.4	7.52×10^{-18}
	231.7	f_1		0.0040	0.5287	29.9	-2.69×10^3	1.28×10^{-4}	94.8	4.81×10^{-18}
	225.3	g_1		0.0020	0.5574	28.3	-4.61×10^3	1.59×10^{-4}	69.0	3.17×10^{-18}
	219.5	h_1		0.0010	0.5819	28.1	-6.63×10^3	1.89×10^{-4}	57.0	2.57×10^{-18}
	214.1	i_1		0.0005	0.6031	28.5	-8.66×10^3	2.18×10^{-4}	50.3	2.30×10^{-18}
	275.7	a_3		0.0150	0.3125	808.8	-2.27×10^{-1}	2.49×10^{-5}	219513.4	5.03×10^{-12}
	273.0	b_3		0.0100	0.3350	59.5	-6.56×10	3.50×10^{-5}	1066.4	1.67×10^{-16}
	271.6	c_3		0.0080	0.3462	44.9	-1.44×10^2	4.08×10^{-5}	564.9	5.45×10^{-17}
300	269.7	d_3	0.0154	0.0060	0.3598	36.8	-2.82×10^2	4.85×10^{-5}	344.4	2.41×10^{-17}
	267.2	e_3		0.0040	0.3772	31.8	-5.28×10^2	5.96×10^{-5}	225.8	1.27×10^{-17}
	263.1	f_3		0.0020	0.4032	29.0	-1.04×10^3	7.87×10^{-5}	151.2	7.54×10^{-18}
	259.2	g_3		0.0010	0.4256	28.6	-1.62×10^3	9.79×10^{-5}	120.9	5.99×10^{-18}
	255.6	h_3		0.0005	0.4451	28.9	-2.23×10^3	1.17×10^{-4}	105.1	5.41×10^{-18}
	291.6	a_{10}		0.0100	0.2127	266.2	-4.43×10^{-1}	1.04×10^{-5}	46862.7	9.54×10^{-14}
	290.8	b_{10}		0.0080	0.2220	76.6	-6.99	1.28×10^{-5}	3661.1	7.18×10^{-16}
	289.8	c_{10}		0.0060	0.2332	46.7	-2.57×10	1.61×10^{-5}	1252.0	1.06×10^{-16}
1000	288.5	d_{10}	0.0108	0.0040	0.2476	35.0	-6.82×10	2.11×10^{-5}	617.8	3.37×10^{-17}
	286.3	e_{10}		0.0020	0.2692	29.5	-1.72×10^2	3.01×10^{-5}	350.6	1.55×10^{-17}
	284.2	f_{10}		0.0010	0.2878	28.4	-2.98×10^2	3.95×10^{-5}	264.7	1.16×10^{-17}
	282.2	g_{10}		0.0005	0.3040	28.6	-4.37×10^2	4.91×10^{-5}	224.7	1.04×10^{-17}

[a] Locations in phase diagram are shown in Figures 8d—8f.

profile of a critical nucleus and its surrounding. PS/CH system is employed as a model system where $X = 500$, $p_1 = 0.642$, $p_2 = 0.190$, entropy parameter $\psi_0 = 0.27$, and Flory theta temperature $\theta = 305.1$ K.[11,12] In the figure, $v_p^0 = 0.0147$, $T_P = 270.22$ K (i.e., $\chi_P^0 = 0.5350$), $v_{p(1)} = 0.001$, $v_{p(2)} = 0.362$, $R = 25.387$, $\Delta f_v = -930\,J\,m^{-3}$, $\Delta t = 0.005\,\mu s$, $D = 2.5 \times 10^{-10}\,m^2\,s^{-1}$, and $\sigma = 5 \times 10^{-6}\,J\,m^{-2}$ (so, $S_{CN} = S_N(0) = 10.75$ nm and $S_0(0) = 32.004$ nm) were assumed. From the figure, the growth of the nucleus $S_N(t)$ and the expansion of the local equilibrium region $S_0(t)$ with time can be readily understood.

Figure 13 shows the effect of σ on the plots of $S_N(t)$ or $S_0(t)$ against t. Under the conditions employed here, critical nuclei grow up after $0.4\,\mu s$ of its birth to a particle with radius of ca. 750 nm and at the same time, the local equilibrium region expands to as wide as ca. 2000 nm, irrespective of σ.

As the nucleus grows in this manner, the surrounding sphere with radius of S_0 also continues to become bigger. During the growth of the nucleus, the outer homogeneous region generates a new critical nucleus (see, Figure 14). Ultimately (at a given time $t = t_p$) the original outer homogeneous phase (hatched area) will disappear completely, due to consumption by continuous expansion of the S_0 sphere and further generation of critical nuclei. All the nuclei (i.e., the particles) at this instant ($t = t_p$) are conventionally defined as primary particles (Figure 14).

We assume that nucleation is always absolutely sporadic and spinodal decomposition is never predominant, then the rate of
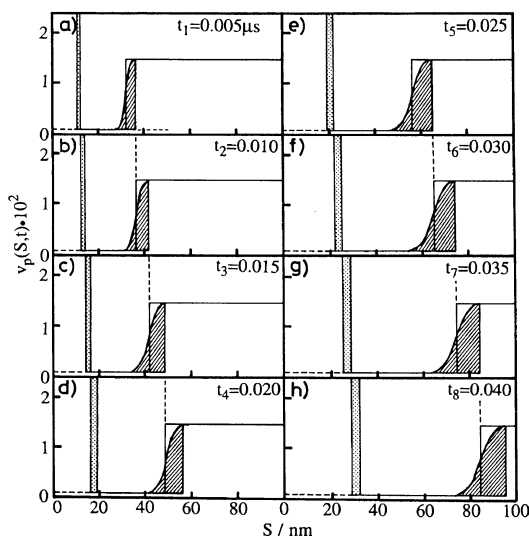
Figure 12. Concentration profile of nucleus and its surroundings together with diffusion $v_p(S, t)$ (hatched area) and increase of radius of nucleus (shadowed area) of polystyrene/cyclohexane system ($X = 500$, $p_1 = 0.642$, $p_2 = 0.190$, $\psi_0 = 0.27$, and $\theta = 305.1$ K): Initial polymer volume fraction, $v_p^0 = 0.0147$; concentration of coexisting phases, $v_{p(1)} = 0.001$ and $v_{p(2)} = 0.362$ (accordingly, $R = 25.387$); difference of free energy between before and after phase separation, $\Delta f_v = -930$ J m^{-3}; phase separation temperature, $T_P = 270.22$ K: Interfacial free energy, $\sigma = 5 \times 10^{-6}$ J m^{-2} [accordingly, $S_{CN} = S_N(0) = 10.75$ nm and $S_0(0) = 32.00$ nm] and diffusion coefficient, $D = 2.5 \times 10^{-10}$ m^2 s^{-2} assumed; a), $t = 0.005\,\mu s$; b), $t = 0.010\,\mu s$; c), $t = 0.015\,\mu s$; d), $t = 0.020\,\mu s$; e), $t = 0.025\,\mu s$; f), $t = 0.030\,\mu s$; g), $t = 0.035\,\mu s$; h), $t = 0.040\,\mu s$.

production of critical nuclei per unit volume is given by

$$\frac{dN_{CN}}{dt} = k_{CN} \exp\left(-\frac{\Delta\phi_{CN}}{k_B T}\right) \qquad (32)$$

with

$$k_{CN} = k'_{CN}\left\{1 - \frac{N_{CN}(t)}{N_{CN}(\infty)}\right\}. \qquad (33)$$

N_{CN} is the number of critical nuclei per unit volume (number m^{-3}), $N_{CN}(t)$, N_{CN} at t, $N_{CN}(\infty)$, N_{CN} at $t = \infty$ and k'_{CN}, the rate constant (number m$^{-3} \cdot$ s^{-1}) and $\Delta\phi_{CN}$ can be calculated using eq 16. Here, nucleation is considered to be described by the same formula as that for the zeroth order reaction. However,
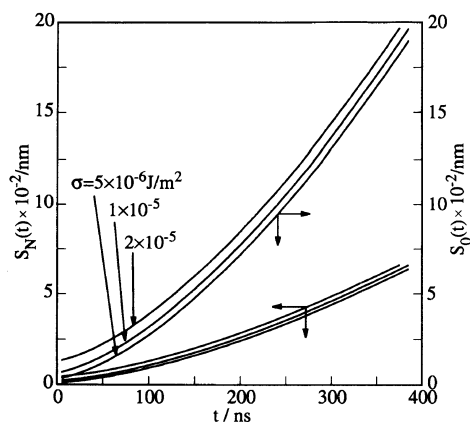

Figure 13. Time dependence of radius of nucleus $S_N(t)$ and that of its surrounding sphere $S_0(t)$ of polystyrene/cyclohexane system ($X = 500$, $p_1 = 0.642$, $p_2 = 0.190$, $\psi_0 = 0.27$, and $\theta = 305.1$ K) : Initial polymer volume fraction, $v_p^0 = 0.0147$; concentration of two coexisting phases, $v_{p(1)} = 0.001$ and $v_{p(2)} = 0.362$ (accordingly, $R = 25.387$); difference of free energy between before and after phase separation, $\Delta f_v = -930$ J m^{-3}; phase separation temperature $T_P = 270.22$ K; interfacial free energy, $\sigma = 5 \times 10^{-6}$ J m^{-2} [accordingly, $S_{CN} = S_N(0) = 10.75$ nm and $S_0(0) = 32.004$ nm], $\sigma = 1 \times 10^{-5}$ J m^{-2} [accordingly, $S_{CN} = 21.505$ nm and $S_0(0) = 64.024$ nm] and $\sigma = 2 \times 10^{-5}$ J m^{-2} [accordingly, $S_{CN} = 43.01$ nm and $S_0(0) = 128.04$ nm]; diffusion coefficient, $D = 2.5 \times 10^{-10}$ m^2 s^{-1}.

the nucleation does not continue without limits as was confirmed repeatedly by a large number of actual experiments if available surveys are to be believed, and it will stop at the instant when the phase equilibrium of total system is realized (*i.e.*, $t = t_P$; see, Figure 14).

Substitution of eq 33 into eq 32 yields

$$\frac{dN_{CN}(t)}{dt} = v\left\{1 - \frac{N_{CN}(t)}{N_{CN}(\infty)}\right\} \qquad (34)$$

with

$$v \equiv k'_{CN} \exp\left(-\frac{\Delta\phi_{CN}}{k_B T}\right). \qquad (35)$$

By solving the differential equation (eq 34), we obtain

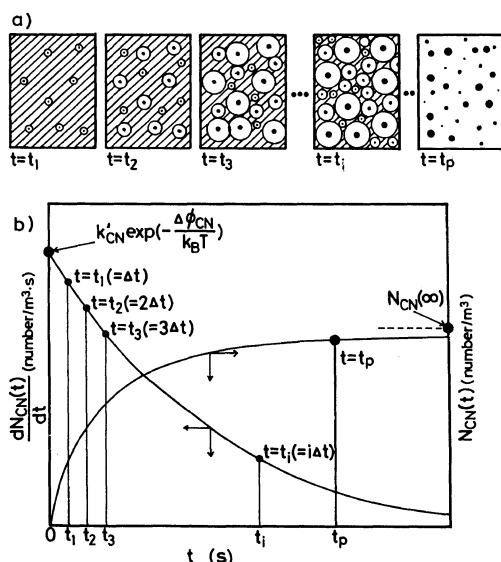$$N_{CN}(t) = N_{CN}(\infty)\left[1 - \exp\left(-\frac{v}{N_{CN}(\infty)}t\right)\right]. \qquad (36)$$

a)

b)

Figure 14. Schematic representation of nucleation and growth of nuclei [a)] and time dependence of nucleation $N_{CN}(t)$ and rate of nucleation dN_{CN}/dt of critical nuclei [b)]: a), ●, nucleus (polymer-rich phase); ○, surrounding sphere (polymer-lean phase); hatched area, outer homogeneous phase.

Combination of eq 34 and 35 gives

$$\frac{dN_{CN}(t)}{dt} = v \exp\left(-\frac{v}{N_{CN}(\infty)}t\right). \quad (37)$$

The total volume of S_0 spheres including growing particles at t, $V_0(t)$ is expressed as

$$V_0(t) = \int_0^t \frac{dN_{CN}(t)}{dt} \frac{4\pi}{3} S_0(t-\tau)^3 d\tau \quad (38)$$

where τ is the time of formation of nucleus and $t-\tau$ is the growing time of nucleus at t. S_0 and S_N are the functions of $t-\tau$ [i.e., $S_0 = S_0(t-\tau)$ and $S_N = S_N(t-\tau)$].

At $t = t_P$, $V(t) = 1$ holds. In other words, in order to estimate t_P, the following equation should be solved.

$$\int_0^{t_P} \frac{dN_{CN}(t)}{dt} \frac{4\pi}{3} S_0(t_P-\tau)^3 d\tau = 1. \quad (39)$$

Since dN_{CN}/dt can be evaluated from $N_{CN}(\infty)$ and v [accordingly, k'_{CN}, $\Delta\phi_{CN}$ and T {see, eq 35}] by eq 37 and $S_0(t-\tau)$ together with

$S_N(t-\tau)$ can be calculated by solving simultaneous equations [eq 24 and 27], t_P can be unambiguously determined by eq 39 under given phase separation conditions. Here, $N_{CN}(\infty)$ (number m^{-3}) should be below the number of polymer molecules (in this case, monodisperse polymer) per unit volume. For example, in the case of the weight fraction of polymer with molecular weight $M = 3 \times 10^4$ g mol^{-1}, $w_X = 0.03$, the following relation

$$N_{CN}(\infty) \leq \frac{w_X \times d_{PL} \times 10^6}{\frac{M}{N_A}} \left(= \frac{0.03 \times 1 \times 10^6}{3 \times 10^4} N_A\right)$$

$$= N_A (= 6.023 \times 10^{23} \text{ number m}^{-3}),$$

$$(40)$$

should be satisfied. Here, d_{PL} is the density of polymer and N_A is Avogadro's constant.

Figure 15 shows the effect of σ and $N_{CN}(\infty)$ on the relations between t_P, obtained by solving an integral equation [eq 39], and k'_{CN} (Figures 15a and 15b) and on the relations between $N_{CN}(t_P)$, calculated by substituting t_P into eq 36, and k'_{CN} (Figures 15c and 15d), respectively. In Figures 15a and 15c, $\Delta\phi_{CN} = 2.42 \times 10^{-21}$ J, (accordingly, $\exp(\Delta\phi_{CN}/k_BT) = 0.523$) was estimated by putting and $\sigma = 5 \times 10^{-5}$ J m^{-2} into eq 16 and Figures 15b and 15d, $\Delta\phi_{CN} = 1.94 \times 10^{-20}$ J (accordingly, $\exp(\Delta\phi_{CN}/k_BT) = 5.56 \times 10^{-3}$) was estimated, in a similar manners from $\sigma = 1 \times 10^{-5}$ J m^{-2} and eq 16. Other conditions are the same as those in Figure 13. At $\sigma = 2 \times 10^{-5}$, $\Delta\phi_{CN} = 1.55 \times 10^{-19}$ J (accordingly, $\exp(\Delta\phi_{CN}/k_BT) = 9.07 \times 10^{-19}$) is obtained and eq 39 can not be solved numerically due to extremely small magnitude of the probability $\exp(\Delta\phi_{CN}/k_BT) = 9.07 \times 10^{-19}$. As k'_{CN} increases t_P decreases monotonically, approaching an asymptotic value which is smaller for larger σ and for larger $N_{CN}(\infty)$. $N_{CN}(t_P)$ increases with k'_{CN}, attaining at $N_{CN}(\infty)$. Figure 15 implies that in a relatively early stage of phase separation all possible nuclei generate completely and thereafter the separation
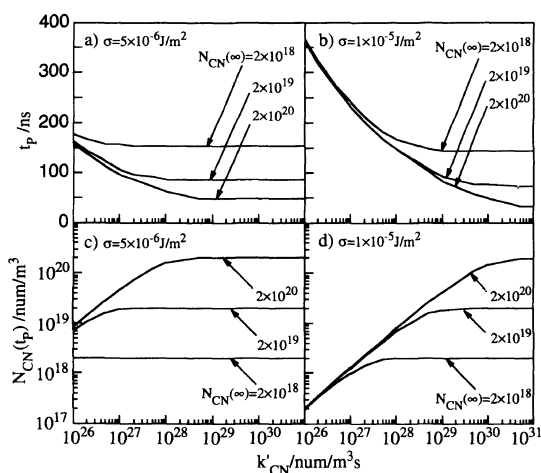
Figure 15. Relations between the time needed for attainment of equilibrium t_P and rate constant of nucleation k'_{CN} (eq 33) [a) and b)] and relations between the nuclei density $N_{CN}(\infty)$ and k'_{CN} [c) and d)] of polystyrene/cyclohexane system: $\sigma = 5 \times 10^{-6} \, J \, m^{-2}$ [a) and c)] and $\sigma = 1 \times 10^{-5} \, J \, m^{-2}$ [b) and d)]; other conditions are the same as those of Figure 13.
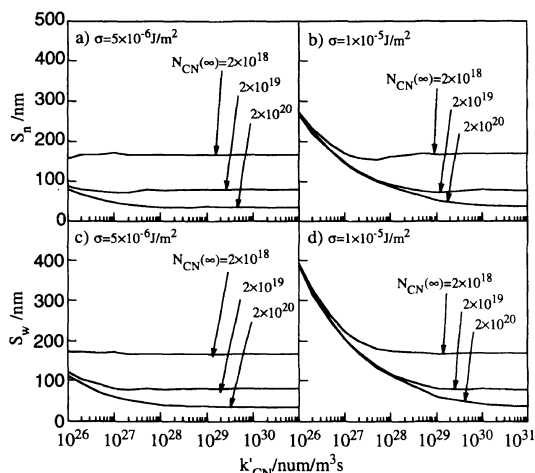

Figure 16. Relations between the number- (or weight-) average radius of the primary particle S_n [a) and b)] (or S_w (c and d)) [*i.e.*, the radius of particles at the time for attainment of phase equilibrium, $t = t_P$] and rate constant of nucleation k'_{CN} for various limiting nuclei density $N_{CN}(\infty)$ of polystyrene/cyclohexane system: $\sigma = 5 \times 10^{-6} \, J \, m^{-2}$ [a) and c)] and $\sigma = 1 \times 10^{-5} \, J \, m^{-2}$ [b) and d)]; other conditions are the same as those of Figure 13.

proceeds by diffusional growth of nuclei.

Figure 16 shows the effect of $N_{CN}(\infty)$ on the relations between the number-average or the
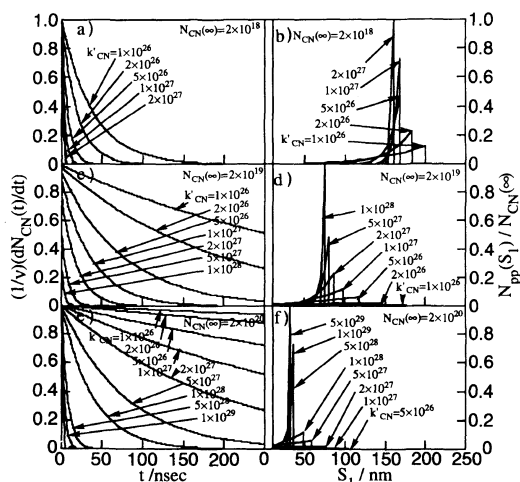

Figure 17. Plots of $(1/v)dN_{CN}/dt$ (eq 37) as a function of time [a), c), and e)] and normalized size distribution of primary particle per unit volume at the time of attainment of equilibrium $t = t_P$ [b), d), and f)], $N_{PP}(S_1)/N_{CN}(\infty)$ for various rate constants k'_{CN} (number $m^{-3} s^{-1}$) of polystyrene/cyclohexane system: $\sigma = 5 \times 10^{-6} \, J \, m^{-2}$; a) and b), $N_{CN}(\infty) = 2 \times 10^{18}$ number m^{-3}; c) and d), $N_{CN}(\infty) = 2 \times 10^{19}$ number m^{-3} and e) and f), $N_{CN}(\infty) = 2 \times 10^{20}$ number m^{-2}; $v = 2.971 \times 10^{25}$ number $m^{-3} s^{-1}$ ($k'_{CN} = 1 \times 10^{26}$), $v = 5.942 \times 10^{25}$ ($k'_{CN} = 2 \times 10^{26}$), $v = 1.486 \times 10^{26}$ ($k'_{CN} = 5 \times 10^{26}$), $v = 2.971 \times 10^{26}$ ($k'_{CN} = 1 \times 10^{27}$), $v = 5.942 \times 10^{26}$ ($k'_{CN} = 2 \times 10^{27}$), $v = 1.486 \times 10^{27}$ ($k'_{CN} = 5 \times 10^{27}$), $v = 2.971 \times 10^{27}$ ($k'_{CN} = 1 \times 10^{28}$), $v = 1.486 \times 10^{28}$ ($k'_{CN} = 5 \times 10^{28}$), $v = 1.486 \times 10^{29}$ ($k'_{CN} = 5 \times 10^{29}$), other conditions are the same as those of Figure 13.

weight-average radius of primary particles (*i.e.*, the particles at t_P) S_n or S_w and k'_{CN}. Here, S_n and S_w are calculated through use of the relations,

$$S_n (\equiv \bar{S}_1) = \frac{\int_0^\infty S_1 N_{PP}(S_1) dS_1}{\int_0^\infty N_{PP}(S_1) dS_1}, \quad (41a)$$

$$S_w = \frac{\int_0^\infty S_1^2 N_{PP}(S_1) dS_1}{\int_0^\infty S_1 N_{PP}(S_1) dS_1}, \quad (41b)$$

where $N_{PP}(S_1)$ (number m^{-4}) is the primary particle radius ($= S_1$) distribution. Particle size distribution $N_{CN}(S_N(t-\tau), t)$ at time t ($0 < \tau < t$)
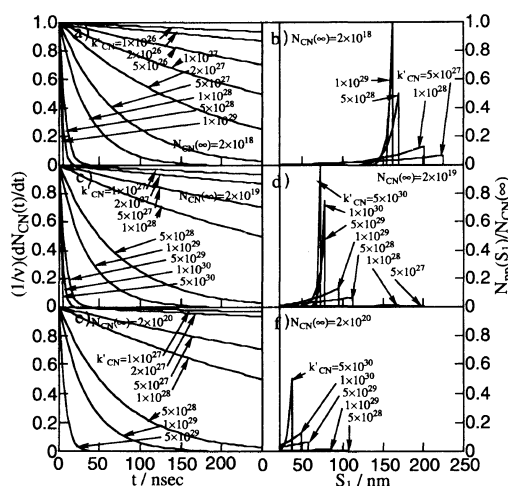
Figure 18. Plots of $(1/v)\,dN_{CN}/dt$ (eq 37) as a function of time [a), c), and e)] and normalized distribution of primary particle per unit volume at $t = t_P$ [b), d), and f)], $N_{PP}(S_1)/N_{CN}(\infty)$ for various rate constant k'_{CN} (number $m^{-3}\,s^{-1}$) of polystyrene/cyclohexane system: $\sigma = 1 \times 10^{-5}$ $J\,m^{-2}$ assumed; other conditions are the same as those of Figure 17.

is given by the following equation,

$$N_{CN}(S_N(t-\tau), t) = v \exp\left(-\frac{v}{N_{CN}(\infty)}\tau\right)$$

$$0 < \tau < t. \qquad (42)$$

Note that $S_N(t-\tau)$ satisfies eq 27. At $t = t_P$, $N_{CN}(S_N(t-\tau), t)$ coincides with $N_{PP}(S_1)$. With an increase in k'_{CN} both S_n and S_w approach their asymptotic values, which strongly depend on $N_{CN}(\infty)$. This means explicitly that S_n and S_w are mainly governed by $N_{CN}(\infty)$, rather than by k'_{CN} for larger k'_{CN}.

Figures 17a, 17c, and 17e ($\sigma = 5 \times 10^{-6}$ $J\,m^{-2}$) and Figures 18a, 18c, and 18e ($\sigma = 1 \times 10^{-5}\,J\,m^{-2}$) show change in $(1/v)dN_{CN}/dt$ (see, eq 37) with time for various combinations of $N_{CN}(\infty)$ and k'_{CN}. In the figure, t_P is indicated as an unfilled circle and $(1/v)dN/dt$ becomes zero beyond t_P. $(1/v)dN_{CN}/dt$ decreases more rapidly with time for larger $N_{CN}(\infty)$ and larger k'_{CN}.

Figures 17b, 17d, and 17f ($\sigma = 5 \times 10^{-6}$ $J\,m^{-2}$) and Figures 18b, 18d, and 18f ($\sigma =$

$1 \times 10^{-5}\,J\,m^{-2}$) show normalized size distribution of the primary particles (i.e., $t = t_P$), $N_{PP}(S_1)/N_{CN}(\infty)$. The mean particle size shifts to smaller S_1 side with an increase in $N_{CN}(\infty)$. Extremely sharp distribution of the primary particles is obtained for larger k'_{CN}, in other words, the primary particles are uniform in size. Lower k'_{CN} yields very broad size distribution of the primary particles, especially for larger σ value (in this case $\sigma = 1 \times 10^{-5}$ $J\,m^{-2}$).

CONCLUSIONS

There are at the initial stage two elementary steps: The nucleation and growth of nuclei by diffusion, which occur concurrently until $t = t_P$. The following conclusions are obtained.

(1) S_{CN} is determined by both σ and Δf_v (eq 15).

(2) Growth rate of nucleus is proportional to $v_p^0 - v_{p(1)}$ and $1/v_{p(2)}$, respectively (eq 28).

(3) Integral equation which determine t_P is suggested (eq 39) and t_P is in the order of 50—500 ns.

(4) Primary particles (PP) are rigorously defined as the nuclei at $t = t_P$ and are proved to be different each other in size depending on the time of nucleation.

(5) The method to calculate distribution of radius of PP, $N_{PP}(S_1)$ is established (eq 42) and $N_{PP}(S_1)$ becomes sharp with the increase of k'_{CN} and with the decrease of $N_{CN}(\infty)$ and σ.

In this article, an isothermal process was treated, but this treatment can readily be generalized to any non-isothermal process.

GLOSSARY OF SYMBOLS

$D = $ diffusion coefficient

$M = $ molecular weight of polymer

$N_A = $ Avogadro's constant

$N_{CN} = $ number of critical nuclei per unit volume (number m^{-3})

$N_{CN}(t) = N_{CN}$ at t

$N_{CN}(\infty) = N_{CN}$ at $t = \infty$

$N_{PP}(S_1)$ = primary particle radius distribution (number m^{-4})

R = phase volume ratio

$\tilde{R}$ = gas constant

S_0 = radius of local equilibrium region

$S_0(t) = S_0$ at t

S_1 = radius of primary particle

S_2 = radius of secondary particle

S_{CN} = radius of critical nucleus

S_N = radius of nucleus

$S_N(t) = S_N$ at t

S_n = number average of S_1

S_w = weight average of S_1

T = Kelvin temperature

T_{CP} = cloud point temperature

T_P = phase separation temperature

V_0 = molar volume of solvent

$V_0(t)$ = total volume of S_0 spheres including growing particles at t

$V_{(1)}$ = volume of polymer-rich phase

$V_{(2)}$ = volume of polymer-lean phase

X = degree of polymerization of polymer

d_{PL} = density of polymer

k_B = Boltzman constant

k_{CN} = rate constant (number m^{-3} s^{-1})

k'_{CN} = rate constant of nucleation

p_1 = 1st order concentration-dependence parameters of χ

p_2 = 2nd order concentration-dependence parameters of χ

t = growing time of nucleus by diffusion

t_P = time at which the phase separation of the whole system is attained

$t_i = i\Delta t$

v_0^0 = initial concentration of solvent

$v_{0(1)}$ = volume fraction of solvent of polymer-lean phase

$v_{0(2)}$ = volume fraction of solvent of polymer-rich phase

v_p^0 = initial (overall) polymer concentration

v_p^c = polymer volume fraction of critical solution point

v_p^s = polymer volume fraction of the starting solution

v_X^0 = initial polymer concentration

v_X^c = critical polymer volume fraction

$v_{X(1)}$ = polymer volume fraction of X-mer of polymer-lean phase in equilibrium

$v_{X(2)}$ = polymer volume fraction of X-mer of polymer-rich phase in equilibrium

$v_{X(1)}^{SP}$ = spinodal concentration of X-mer of polymer-lean phase side

$v_{X(2)}^{SP}$ = spinodal concentration of X-mer of polymer-rich phase side

w_X = weight fraction of X-mer

ΔG_v = Gibbs' free energy change of mixing per unit volume

$\Delta G_v(v_X^0) = \Delta G_v$ at v_X^0

$\Delta \bar{G}(v_X^0)$ = average Gibbs' free energy of coexisting phases A and B

$\Delta V_{p(1)}(t_i)$ = increment of polymer volume in the polymer-lean phase during $t = t_{i-1}$ and $t = t_i$ (given by eq 25)

$\Delta V_{p(2)}(t_i)$ = increment of polymer volume in the polymer-rich phase during $t = t_{i-1}$ and $t = t_i$ (given by eq 26)

Δf_v = free energy change of coagulation per unit volume

Δt = hypothetical time interval of diffusion ($= t_i - t_{i-1}$)

$\Delta \phi(S)$ = activation energy of formation of a nucleus with the radius S

$\Delta \phi_{CN}$ = activation energy of formation of critical nucleus

$\Delta \mu_0$ = chemical potential of solvent

$\Delta \mu_X$ = chemical potential of X-mer

χ = thermodynamic interaction parameter between solvent and polymer

χ_0 = at infinite dilution

$\phi(x)$ = error function

v = rate constant of nucleation

$$\left[= k'_{CN} \exp\left(-\frac{\Delta \phi_{CN}}{k_B T} \right) \right]$$

θ = theta temperature

σ = interfacial energy between the nu-

cleus and its surrounding
τ = time of formation of nucleus
ψ_0 = entropy parameter

REFERENCES

1. R. L. Riley, J. O. Gardner, and U. Merten, *Science*, **143**, 801 (1964).
2. R. D. Schultz and S. K. Asunmaa, "Recent Progress in Surface Science," Vol. 3, J. F. Danielli, A. C. Riddiford, and M. Rosenberg, Ed., Academic Press, New York, N.Y., 1970, pp 291—332.
3. R. E. Kesting and A. Manefee, *Kolloid Z.*, **230**, 241 (1969).
4. C. A. Smolders, "Ultrafiltration Membranes and Applications," A. R. Cooper, Ed., Plenum Press, New York, N.Y., 1980, p 161.
5. W. Pusch and A. Walch, *J. Membrane Sci.*, **10**, 325 (1982).
6. K. Kamide, S. Manabe, T. Matsui, T. Sakamoto, and S. Kajita, *Koubunshi Ronbunshu*, **34**, 205 (1977).
7. K. Kamide and S. Manabe, "Material Science of Synthetic Membranes," ACS Symposium Series, No. 269, D. R. Lloyd, Ed., American Chemical Society, Washington, D.C., 1985, pp 197—228.
8. S. Manabe, Y. Kamata, H. Iijima, and K. Kamide, *Polym. J.*, **19**, 391 (1987).
9. See, for example, J. W. Cahn, *J. Chem. Phys.*, **42**, 93 (1965).
10. K. Kamide, S. Matsuda, T. Dobashi, and M. Kaneko, *Polym. J.*, **16**, 839 (1984).
11. K. Kamide and S. Matsuda, *Polym. J.*, **16**, 825 (1984).
12. K. Kamide, S. Matsuda, and M. Saito, *Polym. J.*, **17**, 1013 (1985).
13. S. Matsuda, *Polym. J.*, **18**, 981 (1986).
14. See, for example, L. Manderkern, "Crystallization of Polymers," McGraw-Hill Book Co., 1964, Chapter 8.
15. See, for example, H. Margenau and G. M. Murphy, "The Mathematics of Physics and Chemistry," D. Van Nostrand Co., 1943, Chapter 7.
16. M. Heinrich and B. A. Wolf, *Polymer*, **33**, 1926 (1992).